NASA CONTRACTOR REPORT

NASA CR-1796

NASA CR-17

SUBSONIC STATIC CHARACTERISTICS OF SLENDER WING CONFIGURATIONS USING A MAGNETIC SUSPENSION AND BALANCE SYSTEM

by Milan Vlajinac, Timothy Stephens, George Gilliam, Nicholas Pertsas, and Eugene Covert

Prepared by
MASSACHUSETTS INSTITUTE OF TECHNOLOGY
Cambridge, Mass. 02139
for Langley Research Center

NATIONAL AERONAUTICS AND SPACE ADMINISTRATION • WASHINGTON, D. C. • JULY 1971

1. Report No. NASA CR-1796	2. Government Accession No.	3. Recipient's Catalog No.
4. Title and Subtitle SUBSONIC STATIC CHARACTERISTICS OF SLENDER WING CONFIGURATIONS USING A MAGNETIC SUSPENSION AND BALANCE SYSTEM		5. Report Date July 1971
		6. Performing Organization Code
7. Author(s) Milan Vlajinac, Timothy Stephens, George D. Gilliam, Nicholas V. Pertsas, and Eugene E. Covert		8. Performing Organization Report No. Technical Report 168
9. Performing Organization Name and Address Massachusetts Institute of Technology Department of Aeronautics and Astronautics Aerospace Research Division Aerophysics Laboratory Cambridge, Massachusetts 02139		10. Work Unit No. 126-63-12-05
		11. Contract or Grant No. NAS1-8658
12. Sponsoring Agency Name and Address National Aeronautics and Space Administration Washington, D. C. 20546		13. Type of Report and Period Covered Contractor Report
		14. Sponsoring Agency Code
15. Supplementary Notes		

16. Abstract

Aerodynamic forces and moments on three low-aspect-ratio wing planforms were obtained using a magnetic suspension and balance system. Comparison of the present data with both theory and experimental results obtained elsewhere is presented and shown to be in close agreement.

17. Key Words (Suggested by Author(s)) Wind tunnel; Magnetic suspension; Magnetic balance; Aerodynamics; Slender wings		18. Distribution Statement Unclassified - Unlimited	
19. Security Classif. (of this report) Unclassified	20. Security Classif. (of this page) Unclassified	21. No. of Pages 25	22. Price* $3.00

*For sale by the National Technical Information Service, Springfield, Virginia 22151

SUBSONIC STATIC CHARACTERISTICS OF SLENDER WING CONFIGURATIONS USING A MAGNETIC SUSPENSION AND BALANCE SYSTEM

By Milan Vlajinac, Timothy Stephens, George Gilliam,
Nicholas Pertsas, Eugene Covert
Massachusetts Institute of Technology

SUMMARY

Wind tunnel investigation of the static aerodynamic characteristics of three sharp-edged, slender wings were conducted at subsonic speeds using a magnetic suspension and balance system. Measurements of lift, drag, and pitching moment coefficients were made at angles of attack from 2° to 30° at a Reynolds number of the order of 1×10^5 and a Mach number of approximately 0.05.

The results were expected to be relatively free from Reynolds number effects due to the sharp leading and trailing edges of these wing planforms, and therefore in agreement with larger scale data.

Comparison of the present results is made with previously published experimental data, as well as with a theoretical model using the leading-edge suction analogy.

The agreement of the present results with data obtained at test Reynolds numbers an order of magnitude larger is considered good, thereby validating the small scale tests.

INTRODUCTION

In recent years, the trend in wing design for application to supersonic aircraft has been toward planforms of low aspect ratio and large leading edge sweep angle. In particular, the delta wing and related wings with sharp leading edges have been the subject of considerable theoretical and experimental investigations. Application of simple potential flow theory has proven to be inadequate in predicting the aerodynamic characteristics of these wings, since the flow over such wings at moderate angle of attack is characterized at subsonic speeds by the formation of leading edge separation vortices. Associated with these vortices is an increase in both the lift and drag of the wing over the potential-flow case.

In view of the current interest in low aspect ratio planforms, an experimental study was undertaken at the M.I.T. Aerophysics Laboratory to obtain the static force and moment characteristics of three related delta wing configurations at low Mach number. The tests involved the use of a magnetic suspension and balance system*. The primary purpose of these tests was to explore the ability of the magnetic balance to provide aerodynamic data on wing model (non-axisymmetric) configurations at high angles of attack and compare this data with both available experimental results, and current theoretical methods. Although the magnetic suspension technique is particularly desirable for testing aerodynamic configurations where support interference effects are significant, this was not the motivation for the tests described herein. In fact, the particular configurations chosen were likely to be relatively free of unpredictable sting interference effects. Consequently, comparison with similar data obtained with sting-supported models was expected to be close. Due to the sharp edges of these planforms, separation occurs at the leading edge and the results should, therefore, not be subject to Reynolds number effects. This should reduce the problems of comparing the present results at low Reynolds numbers with data obtained in larger-scale tests.

---

*This balance was developed under sponsorship of the NASA-Langley Research Center and is described in Reference 1. The power supplies were developed under sponsorship of ARL. The authors thank Mr. Fred Daum of ARL for permission to use them in this Program.

SYMBOLS

A	Wing aspect ratio, b^2/S
b	Wing span
c	Wing chord
$\bar{c}$	Mean aerodynamic chord, $(\frac{2}{S}\int_0^{b/2} c^2 dy)$
C_D	Drag coefficient $(\frac{Drag}{qS})$
C_{D_o}	Drag coefficient at $\alpha = 0$
C_L	Lift coefficient $(\frac{Lift}{qS})$
C_M	Pitching moment coefficient $(\frac{\text{Pitching moment}}{qS\bar{c}})$
$\ell_{1/4}$	Quarter chord point of the mean aerodynamic chord
M	Mach number
q	Dynamic pressure
$Re_{\bar{c}}$	Reynolds number based on mean aerodynamic chord
S	Wing planform area
X_{c_p}	Center of pressure location measured from wing apex
α	Angle of attack, degrees

CHAPTER I

APPARATUS

Magnetic Balance Description

The magnetic balance used in these tests is described in detail in Reference 1. The balance is presently capable of magnetically suspending a variety of ferromagnetic model geometries and measuring five components of force and moment on the model (excluding rolling moment). The forces and moments are computed from the measured magnet coil currents required to balance the aerodynamic and gravity loads. The measured magnet currents, tunnel conditions and model position data are processed by a computer program which reduces the data to aerodynamic coefficient form. The data reduction techniques developed for this balance are discussed in detail in Reference 2.

Subsonic Wind Tunnel

The subsonic wind tunnel used in these tests was designed for use in conjunction with the magnetic balance system described earlier. It is an open circuit, closed jet tunnel with intake open to the test room. A continuous variation in velocity from 0 to 550 ft./sec. can be obtained at the test section. This corresponds to a maximum dynamic pressure of 360 pounds per square foot and freestream Reynolds number of 3.5×10^6/per foot. The test section is octagonal with inside dimensions of 6 1/4 inches.

Model Description

The models used in these tests were three 74° leading edge sweep planforms. The model details are shown in Figure 1. The wings were machined from fiber glass sheet stock. The body cores for the wings were machined from as-received Armco magnetic ingot iron. The machined slots in the model cores permitted the same core to be used with all three wing configurations.

CHAPTER II

DESCRIPTION OF TESTS

Wind Tunnel Conditions

Subsonic tests were conducted on the three configurations described to obtain the static lift, drag and pitching moment coefficients over an angle of attack range from 2° to 30°. These models possess an aerodynamic roll stiffness at angles of attack other than zero degrees. In view of this fact, and since no magnetic control of the roll degree of freedom was available in these tests, all the data obtained were for non-zero angles.

The nominal tunnel conditions in these tests were a Mach number of 0.05 and a freestream Reynolds number of 4.0×10^5 per foot.

Data Acquisition and Procedures

The static forces and moments were obtained by measuring the magnet coil currents required to balance gravity and aerodynamic loads on the models. The magnet currents were measured with an integrating digital voltmeter. Integration (averaging) period for each current measurement was 10 seconds. Voltmeter readings were recorded with a digital printer. The 10 second sampling attenuates the effects of ripple and noise and provides an accurate average of the coil current from which the steady state loads on the model can be obtained.

The model position with respect to the wind tunnel axis was visually monitored and set with three transits. The model absolute position and orientation was measured to the following estimated accuracy.

Translations (Lift, Drag, Slip): ±0.001 in.

Angles (Pitch, Yaw): ±0.1°

The procedures used for each data point were the following:

1. The desired model position with respect to the tunnel was indexed on the transits. The model was then translated and rotated to this position with the magnetic balance position control (see Reference 1).

2. The wind tunnel static pressure and temperature were recorded.

3. The six magnet currents were sampled for 10 seconds each and recorded.

4. The model position was checked to insure no change in position had occurred.

5. The procedure was returned to Step 1.

A similar procedure as outlined above was repeated wind-off with the omission of Step 2 at each model position for which wind-on data had been taken. This provided the tare currents which were required in the data reduction process.

The resulting magnet currents, model position and tunnel conditions were processed by a computer program to reduce the data to aerodynamic coefficient form.

The data were corrected for tunnel blockage and wing induced downwash using the methods described in Reference 3.

Test Results and Discussion

The drag, lift and pitching moment coefficients obtained for the three wing configurations are shown in Table 1. The moment coefficients are referred to the wing apex. The center of pressure location for the wings relative to the mean quarter chord point are tabulated in non-dimensional form.

The lift and drag coefficients are non-dimensionalized with the wing planform area and the moment coefficients are non-dimensional with the mean aerodynamic chord as the reference length.

The lift coefficient versus angle of attack for the models tested is shown in Figure 2. A relatively small difference in lift characteristics was observed between the three planforms.

The drag coefficient versus angle of attack is shown in Figure 3 and, like the lift characteristics shown in Figure 2, the drag coefficient also shows only small variation for the models tested.

The measured pitching moment coefficient versus angle of attack is shown in Figure 4. An increase in pitching moment slope with angle of attack is observed as the wing aspect ratio increases. The center of pressure for all three configurations appears to lie slightly aft of the mean quarter chord point and is shown in Figures 5, 6 and 7. A small variation in the center of pressure location with angle of attack is indicated.

Comparison of present lift coefficient data versus angle of attack for the delta wing planform with both theoretical and experimental results obtained elsewhere is shown in Figure 8. The lift coefficient versus angle of attack for a delta wing with 74° leading edge sweep using the method developed in Reference 4 is shown as well as the experimental values obtained in reference 5 for a delta wing with 75° leading edge sweep. The present data shows a lower value of lift coefficient than predicted by both Polhamus's theory and the experimental results of Reference 5. A possible cause for the lower values of the lift coefficient in the present study could be due to the model body extending aft of the wing trailing edge (see Figure 1), thereby being in the downwash from the wing. This explanation is consistent with the behavior of the pitching moment curve in Figure 9. The agreement of the present lift coefficient data with that obtained in Reference 5 is within 2%, in spite of an order of magnitude difference between the two test Reynolds numbers.

The present delta wing drag coefficient data plotted as drag due to lift ($C_D - C_{D_o}$) versus angle of attack is compared in Figure 10 with results obtained in reference 5 for a 72.5° and 75° sweep delta wing. The present results (74° sweep wing) are seen to fall between the Reference 5 curves. It should again be emphasized that though the present test Reynolds number was an order of magnitude smaller, the data appear to agree with the larger scale results.

The lift coefficient data versus angle of attack for the diamond wing model is compared in Figure 11 with Polhamus' theory from Reference 6. The agreement here is within 3%. The diamond model body did not extend beyond the trailing edge of the wing as in the case of the delta wing model (Figure 1). This could explain the closer agreement of Polhamus' method with the present diamond wing than with the delta wing results (see Figure 8).

CHAPTER III

CONCLUSIONS

Subsonic aerodynamic forces and moments over an angle of attack range of 30° were obtained on three low aspect ratio wing planforms using a magnetic suspension and balance system. Comparison of the present delta wing data is made with experimental data obtained in other investigations. The agreement of the present data with results obtained at a factor of 10 higher test Reynolds number is considered good. The lower values for lift coefficient (∿6%) obtained here appear to be due to the model body extending aft of the wing trailing edge and thereby being in the wing downwash.

Comparison of the present data with Polhamus' theory is shown to be in close agreement (∿3%) for the diamond wing planform. In the case of the delta wing, the discrepancy (∿6%) between the thoery and present results could again be an effect of the model body extending aft of the wing trailing edge.

REFERENCES

1. Stephens, T., "Design, Construction, and Evaluation of a Magnetic Suspension and Balance System for Wind Tunnels," NASA CR-66903, Nov. 1969.

2. Gilliam, G. D., "Data Reduction Techniques for Use with a Wind Tunnel Magnetic Suspension and Balance System," Mass. Inst. of Tech., TR 167, June 1970.

3. Pope, Alan, Wind Tunnel Testing, John Wiley and Sons, November 1958.

4. Polhamus, E. C., "A Concept of the Vortex Lift of Sharp-Edge Delta Wings Based on a Leading-Edge-Suction Analogy," NASA TN D-3767, 1966.

5. Polhamus, E.C., "Predictions of Vortex Lift Characteristics Based on a Leading-Edge Suction Analogy," AIAA Paper 69-1133, 1969.

6. Wentz, H. W., Kohlman, D. L., "Wind Tunnel Investigations of Vortex Breakdown on Slender Sharp-Edge Wings, NASA CR-98737, Nov., 1968.

7. Peckham, D. H., "Low-Speed-Wind-Tunnel Tests on a Series of Uncambered Slender Pointed Wings with Sharp Edges," R & M NO. 3186, Brit, A.R.C., 1961.

TABLE I

ARROW - WING

α°	M	$Re_{\bar{c}}$ x10^{-5}	C_D	C_L	C_M	$\frac{X_{cp}-\ell_{1/4}}{\bar{c}}$
2	0.0564	0.7543	0.0213	0.0409	-0.0429	0.1616
4	0.0560	0.7490	0.0282	0.1046	-0.1054	0.1214
4	0.0563	0.7523	0.0282	0.1021	-0.0998	0.0912
6	0.0557	0.7452	0.0394	0.1647	-0.1558	0.0582
8	0.0553	0.7403	0.0573	0.2387	-0.2276	0.0617
8	0.0553	0.7396	0.0571	0.2360	-0.2245	0.0592
10	0.0552	0.7388	0.0789	0.3113	-0.3076	0.0907
10	0.0548	0.7324	0.0785	0.3100	-0.3005	0.0725
12	0.0549	0.7343	0.1093	0.3832	-0.3698	0.0605
12	0.0543	0.7265	0.1114	0.3898	-0.3582	0.0159
14	0.0543	0.7266	0.1513	0.4753	-0.4631	0.0606
16	0.0539	0.7208	0.2015	0.5566	-0.5111	-0.0045
16	0.0540	0.7222	0.1953	0.5455	-0.4910	-0.0206
16	0.0538	0.7190	0.2008	0.5555	-0.5088	-0.0064
18	0.0536	0.7174	0.2493	0.6364	-0.6314	0.0556
20	0.0529	0.7077	0.3204	0.7340	-0.7355	0.0503
20	0.0530	0.7086	0.3111	0.7233	-0.7105	0.0340
22	0.0523	0.6992	0.3870	0.8085	-0.8259	0.0533
24	0.0512	0.6848	0.4551	0.8862	-0.9040	0.0390
24	0.0514	0.6869	0.4508	0.8758	-0.8930	0.0382
26	0.0490	0.6553	0.5673	1.0068	-1.0651	0.0535
28	0.0488	0.6528	0.6360	1.0461	-1.1513	0.0721
28	0.0489	0.6541	0.6317	1.0338	-1.1377	0.0709
30	0.0479	0.6406	0.7398	1.1192	-1.2879	0.0919

TABLE I - Continued

DIAMOND - WING

$\alpha°$	M	$Re_{\bar{c}} x10^{-6}$	C_D	C_L	C_M	$\frac{X_{cp} - \ell_{1/4}}{\bar{c}}$
4	0.0560	0.1117	0.0219	0.0950	-0.0727	0.0864
4	0.0551	0.1097	0.0213	0.1002	-0.0805	0.1251
4	0.0547	0.1091	0.0207	0.0960	-0.0738	0.0905
6	0.0564	0.1124	0.0310	0.1477	-0.1133	0.0864
6	0.0556	0.1107	0.0320	0.1561	-0.1224	0.1030
8	0.0550	0.1095	0.0481	0.2175	-0.1641	0.0705
8	0.0541	0.1078	0.0472	0.2155	-0.1608	0.0624
8	0.0536	0.1068	0.0465	0.2123	-0.1563	0.0528
10	0.0546	0.1087	0.0683	0.2767	-0.2020	0.0418
10	0.0544	0.1084	0.0706	0.2841	-0.2127	0.0594
12	0.0540	0.1075	0.1003	0.3569	-0.2652	0.0480
12	0.0525	0.1045	0.0972	0.3510	-0.2574	0.0393
14	0.0535	0.1065	0.1381	0.4323	-0.3222	0.0428
14	0.0520	0.1036	0.1352	0.4282	-0.3159	0.0363
14	0.0522	0.1039	0.1343	0.4277	-0.3152	0.0357
16	0.0517	0.1030	0.1840	0.5158	-0.3875	0.0404
18	0.0512	0.1020	0.2408	0.6072	-0.4609	0.0383
18	0.0512	0.1020	0.2395	0.6022	-0.4527	0.0313
20	0.0503	0.1002	0.3046	0.6940	-0.5346	0.0381
22	0.0490	0.0978	0.3744	0.7787	-0.6082	0.0367
22	0.0491	0.0978	0.3770	0.7833	-0.6129	0.0378
24	0.0482	0.0960	0.4555	0.8742	-0.7030	0.0458
26	0.0475	0.0947	0.5364	0.9594	-0.7802	0.0422
26	0.0476	0.0950	0.5360	0.9491	-0.7757	0.0442
28	0.0469	0.0935	0.6347	1.0393	-0.8738	0.0502

TABLE I - Concluded

DELTA - WING

$\alpha°$	M	$Re_{\bar{c}} \times 10^{-5}$	C_D	C_L	C_M	$\frac{X_{cp} - \ell_{1/4}}{\bar{c}}$
2	0.0560	0.9315	0.0168	0.0494	-0.0447	0.1438
4	0.0546	0.9098	0.0252	0.0991	-0.0834	0.0792
4	0.0555	0.9236	0.0244	0.1062	-0.0960	0.1420
4	0.0557	0.9266	0.0244	0.1069	-0.0971	0.1465
6	0.0548	0.9141	0.0353	0.1587	-0.1315	0.0644
8	0.0546	0.9102	0.0520	0.2306	-0.1960	0.0821
8	0.0547	0.9103	0.0522	0.2335	-0.1976	0.0790
10	0.0539	0.8987	0.0767	0.3056	-0.2589	0.0742
12	0.0535	0.8922	0.1100	0.3878	-0.3313	0.0741
12	0.0538	0.8949	0.1083	0.3827	-0.3220	0.0618
12	0.0535	0.8910	0.1092	0.3888	-0.3290	0.0667
14	0.0532	0.8853	0.1481	0.4656	-0.3956	0.0616
16	0.0528	0.8794	0.1986	0.5576	-0.4798	0.0625
16	0.0527	0.8775	0.1948	0.5522	-0.4680	0.0510
18	0.0523	0.8706	0.2555	0.6483	-0.5585	0.0533
18	0.0522	0.8687	0.2550	0.6453	-0.5555	0.0524
20	0.0516	0.8587	0.3194	0.7372	-0.6355	0.0428
20	0.0516	0.8587	0.3182	0.7342	-0.6347	0.0450
22	0.0503	0.8374	0.4138	0.8415	-0.7569	0.0596
24	0.0491	0.8176	0.4735	0.9188	-0.8181	0.0431
24	0.0492	0.8192	0.4784	0.9165	-0.8255	0.0504
26	0.0483	0.8049	0.5754	1.0122	-0.9513	0.0690
26	0.0484	0.8056	0.5613	0.9982	-0.9251	0.0595
28	0.0478	0.7965	0.6517	1.0817	-1.0316	0.0683

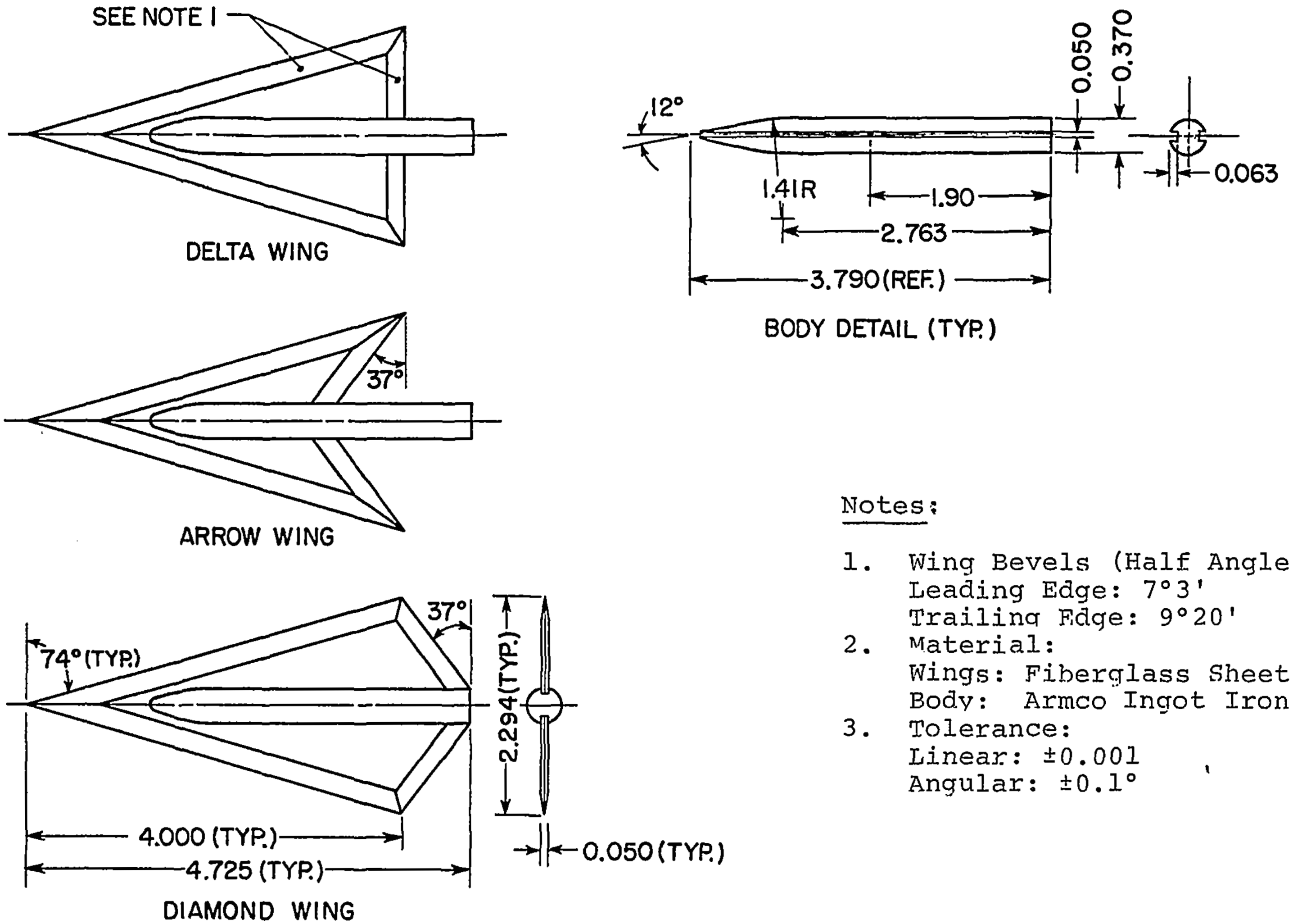

Notes:

1. Wing Bevels (Half Angle):
   Leading Edge: 7°3'
   Trailing Edge: 9°20'
2. Material:
   Wings: Fiberglass Sheet
   Body: Armco Ingot Iron
3. Tolerance:
   Linear: ±0.001
   Angular: ±0.1°

Figure 1. MODEL CONFIGURATIONS

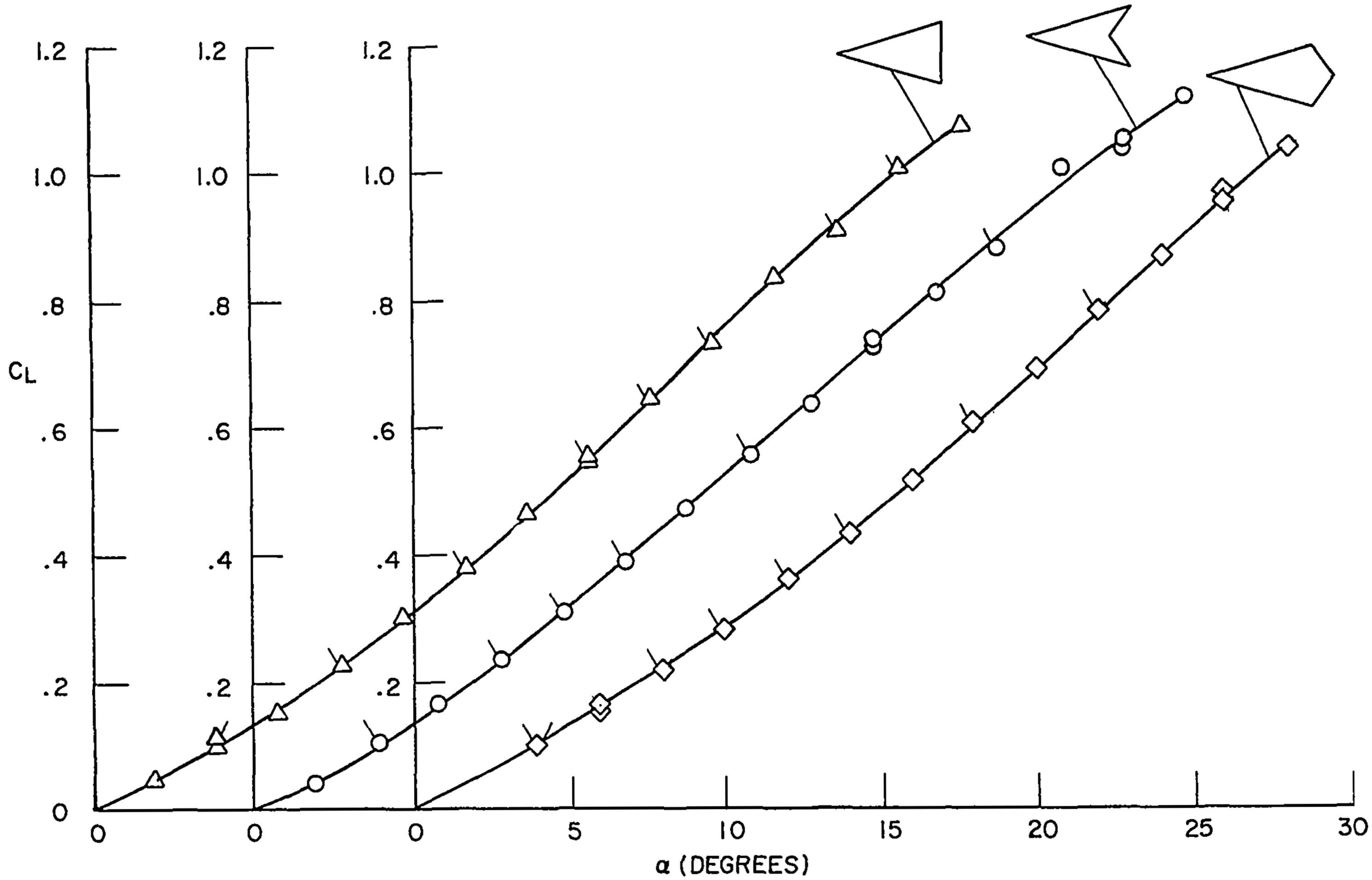

Figure 2. LIFT COEFFICIENT VERSUS ANGLE OF ATTACK

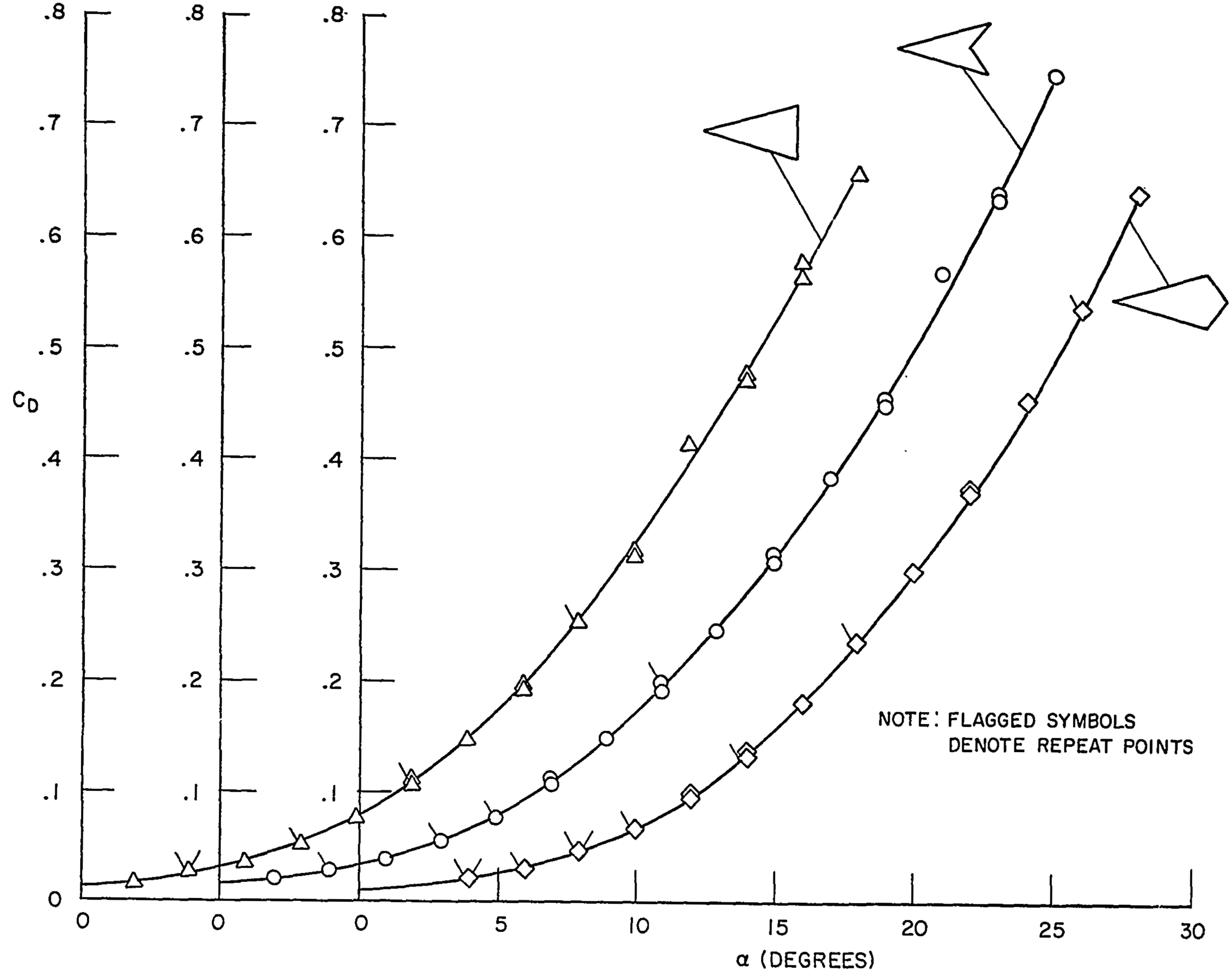

Figure 3. DRAG COEFFICIENT VERSUS ANGLE OF ATTACK

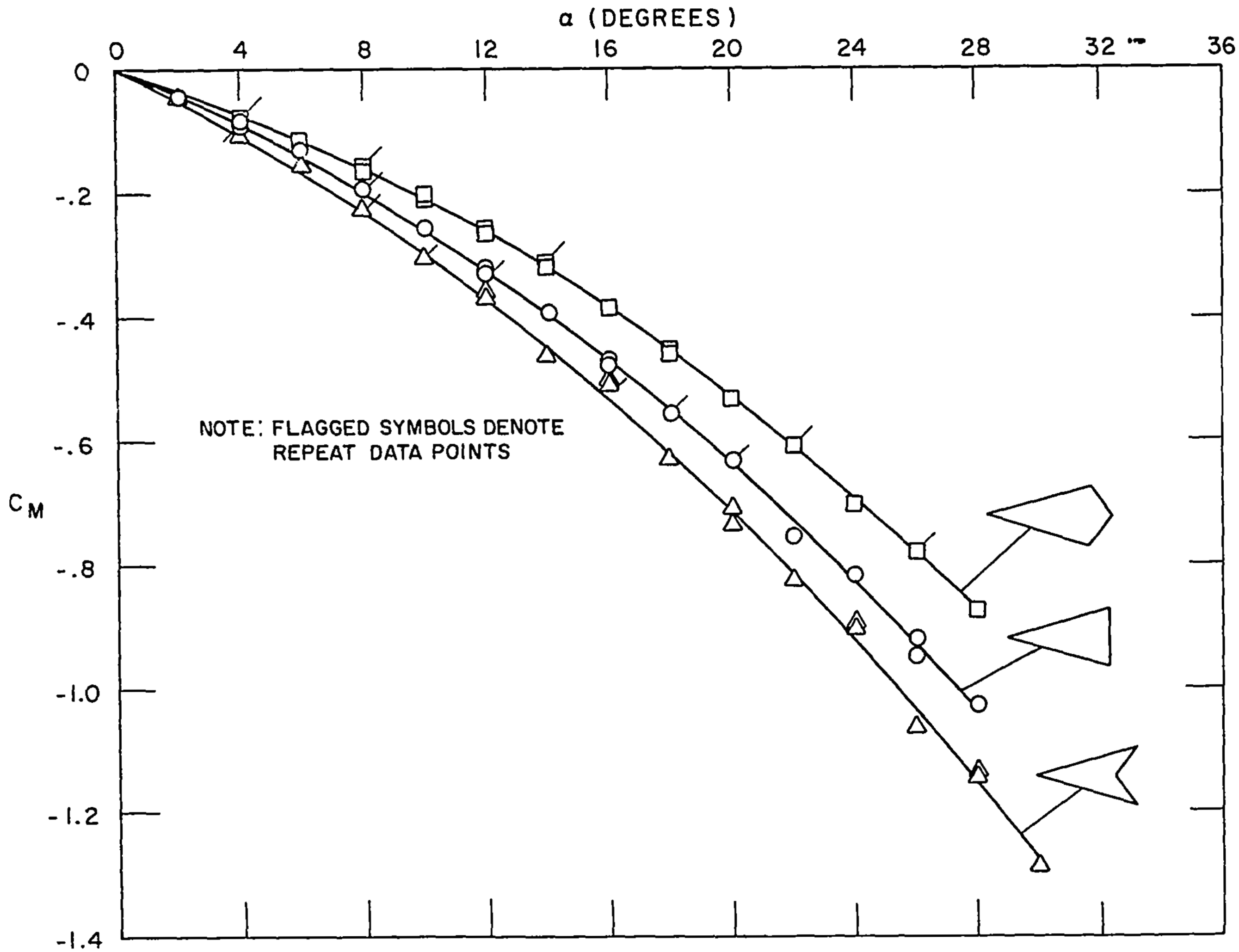

Figure 4. PITCHING MOMENT VERSUS ANGLE OF ATTACK

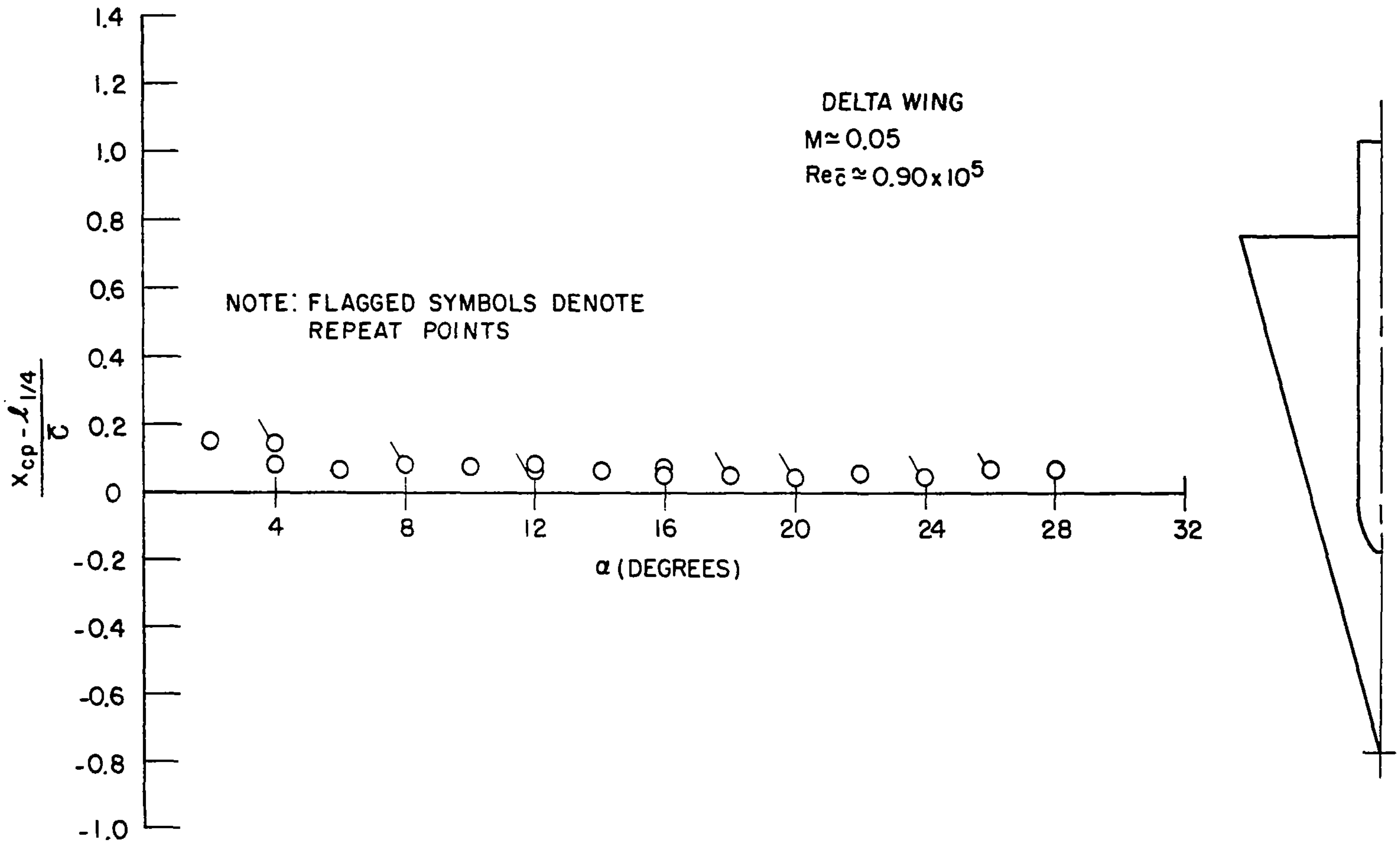

Figure 5. CENTER OF PRESSURE LOCATION VERSUS ANGLE OF ATTACK

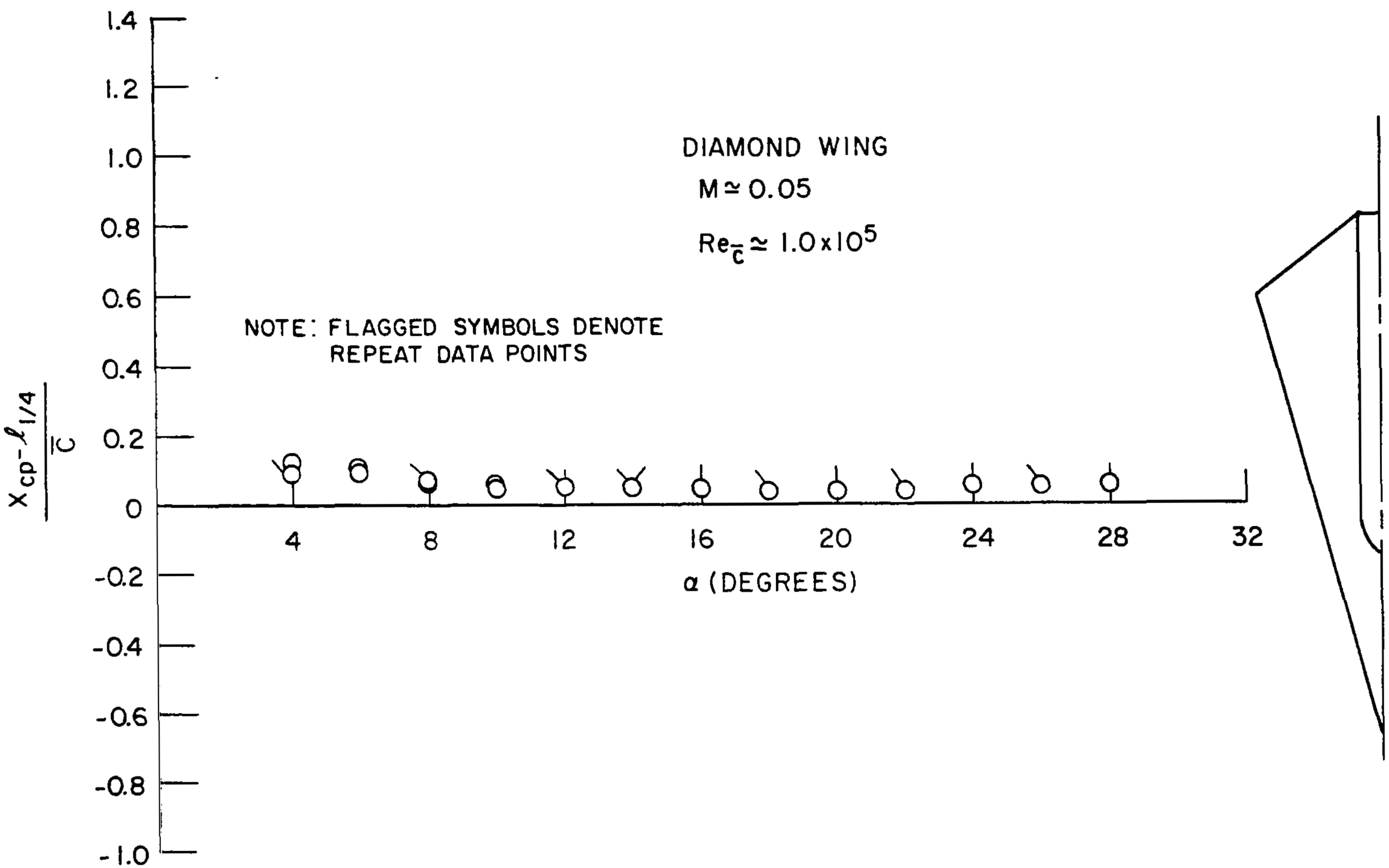

Figure 6. CENTER OF PRESSURE LOCATION VERSUS ANGLE OF ATTACK

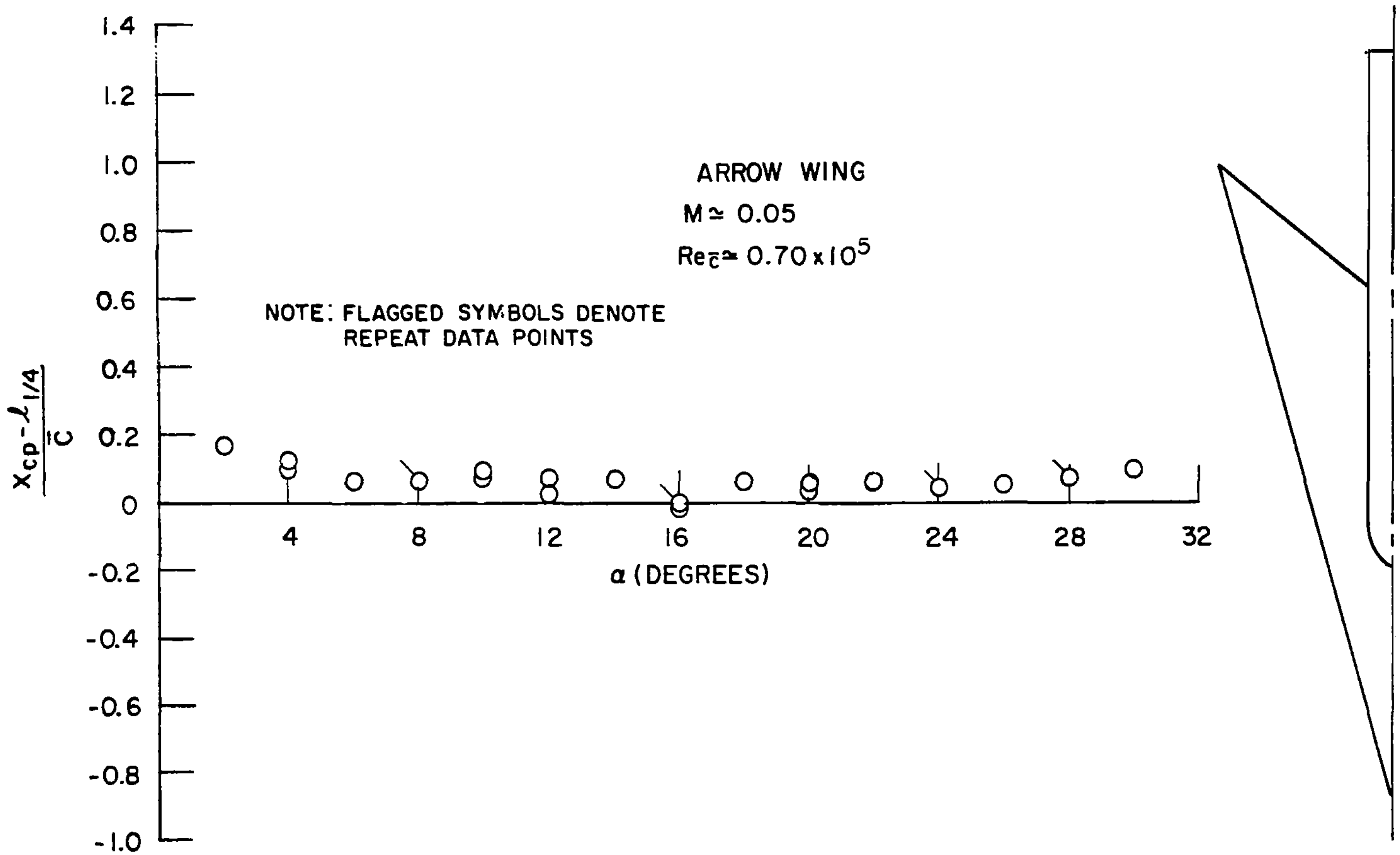

Figure 7. CENTER OF PRESSURE LOCATION VERSUS ANGLE OF ATTACK

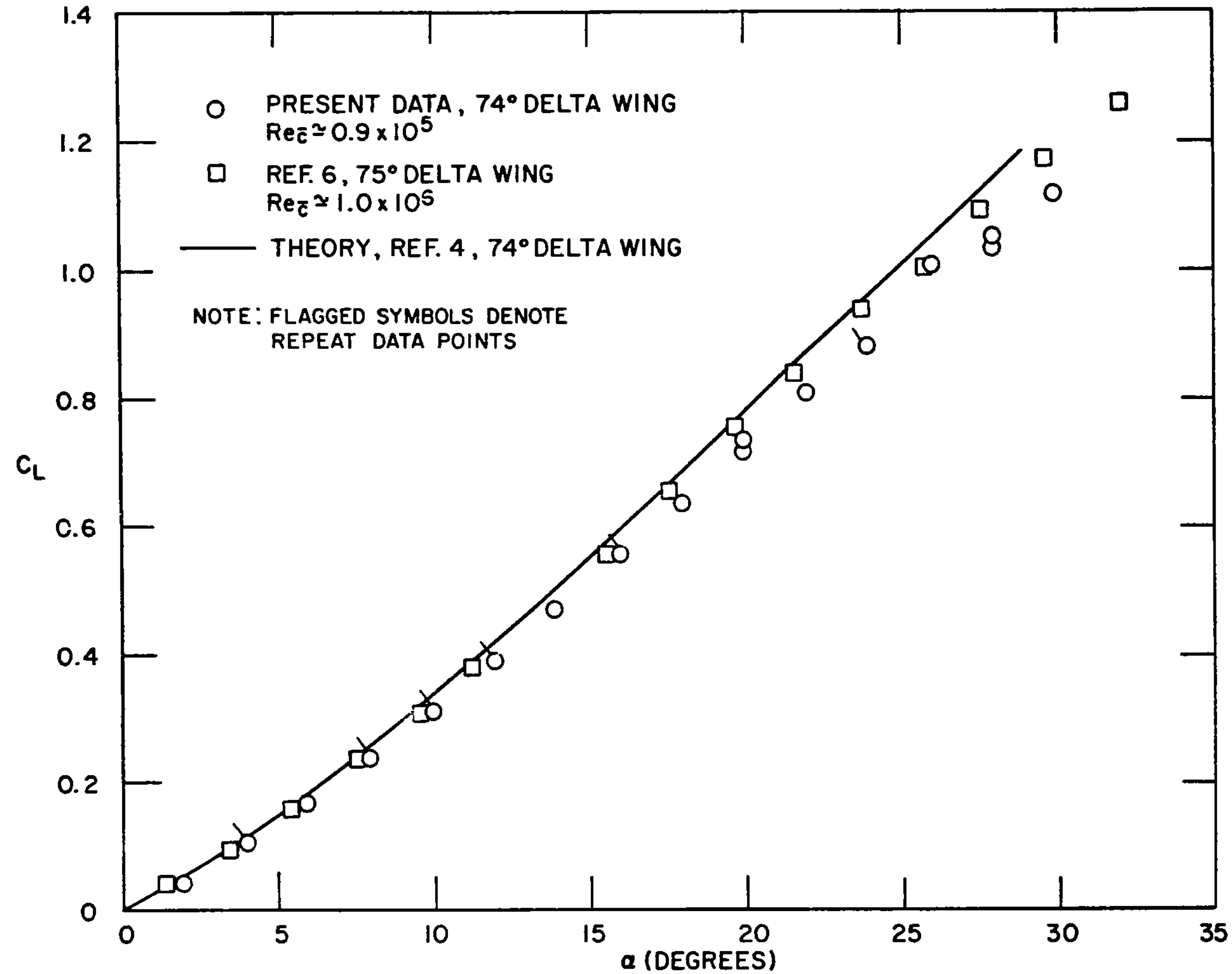

Figure 8. LIFT COEFFICIENT VERSUS ANGLE OF ATTACK

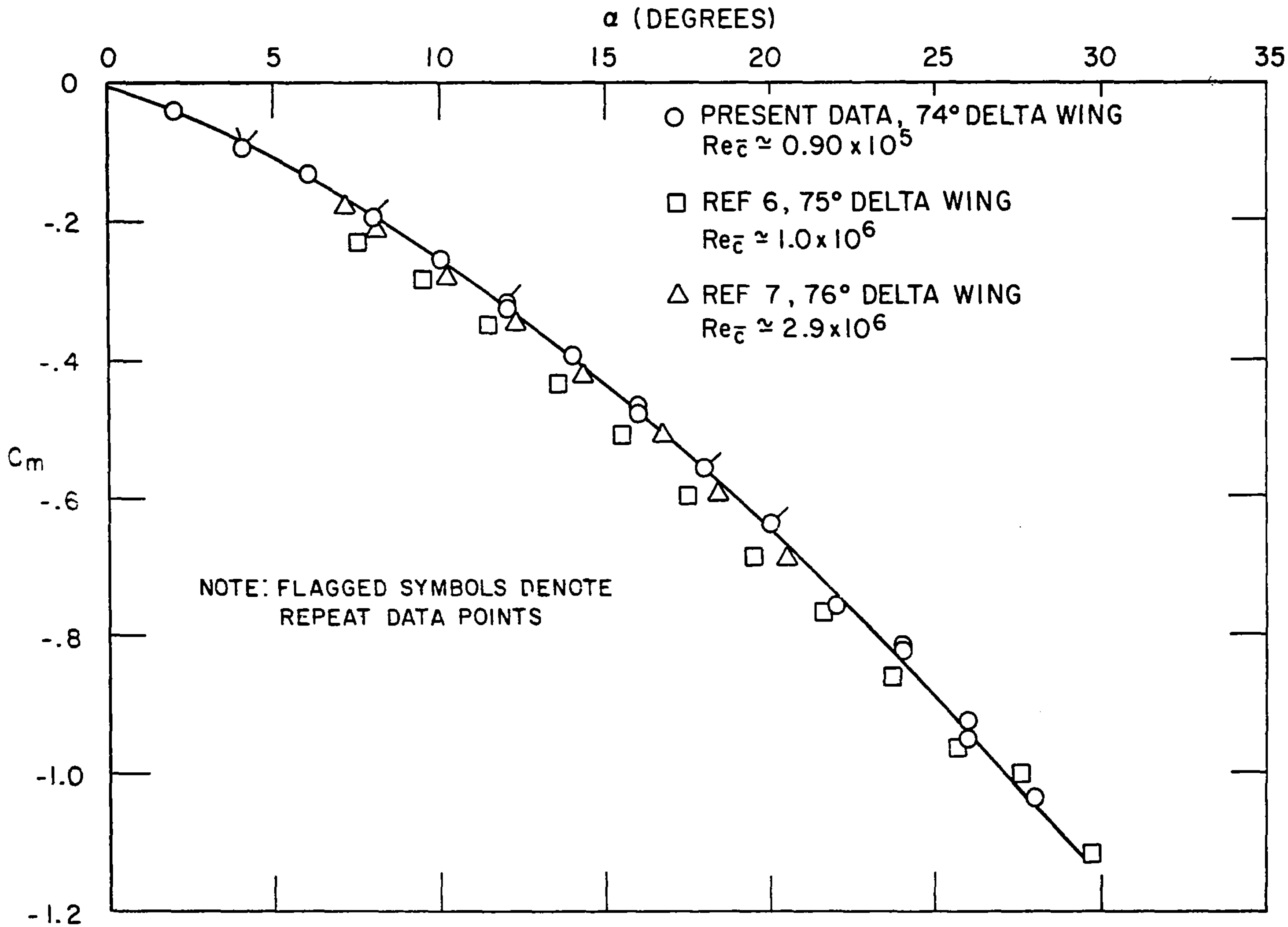

Figure 9. PITCHING MOMENT COEFFICIENT VERSUS ANGLE OF ATTACK

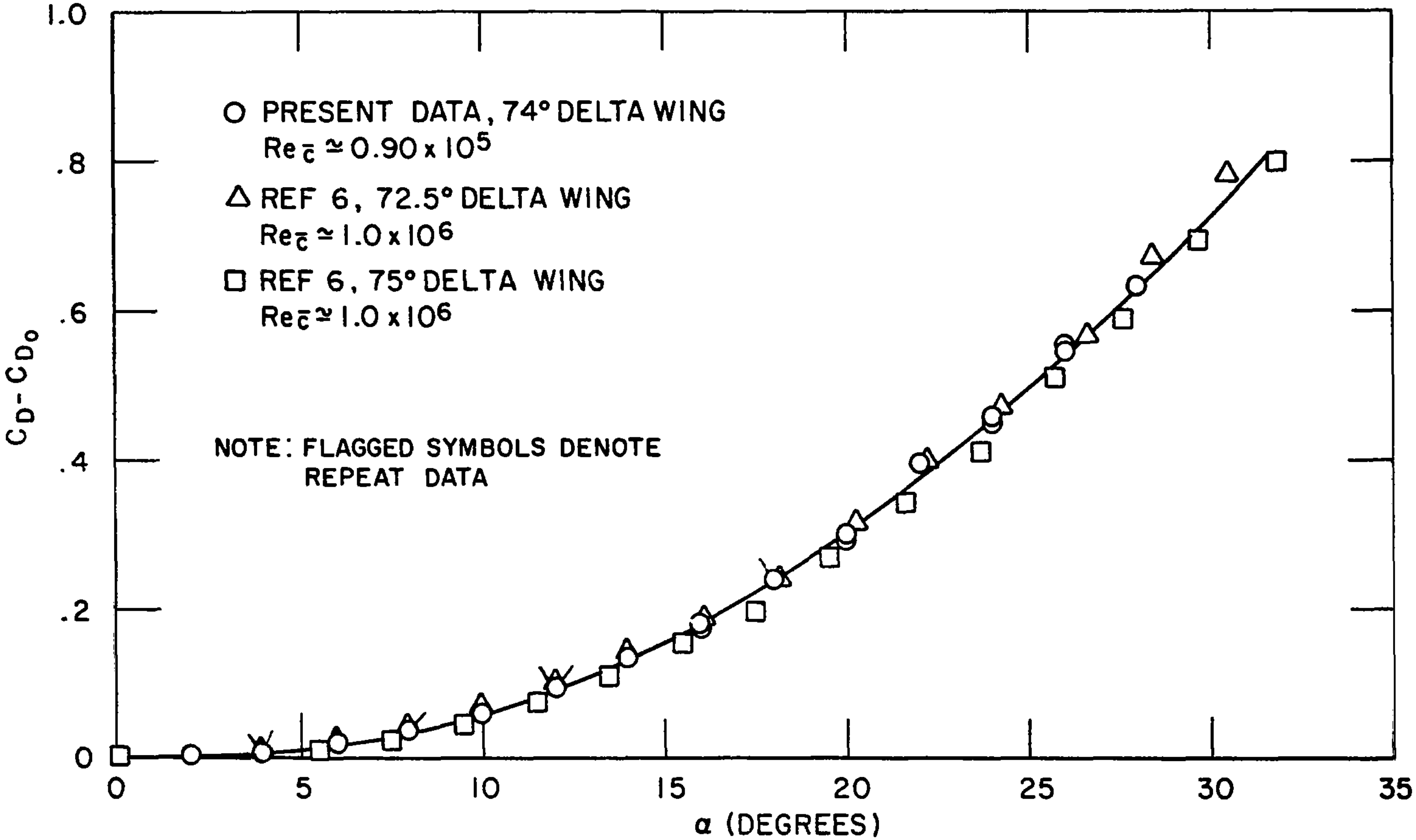

Figure 10. INDUCED DRAG COEFFICIENT VERSUS ANGLE OF ATTACK

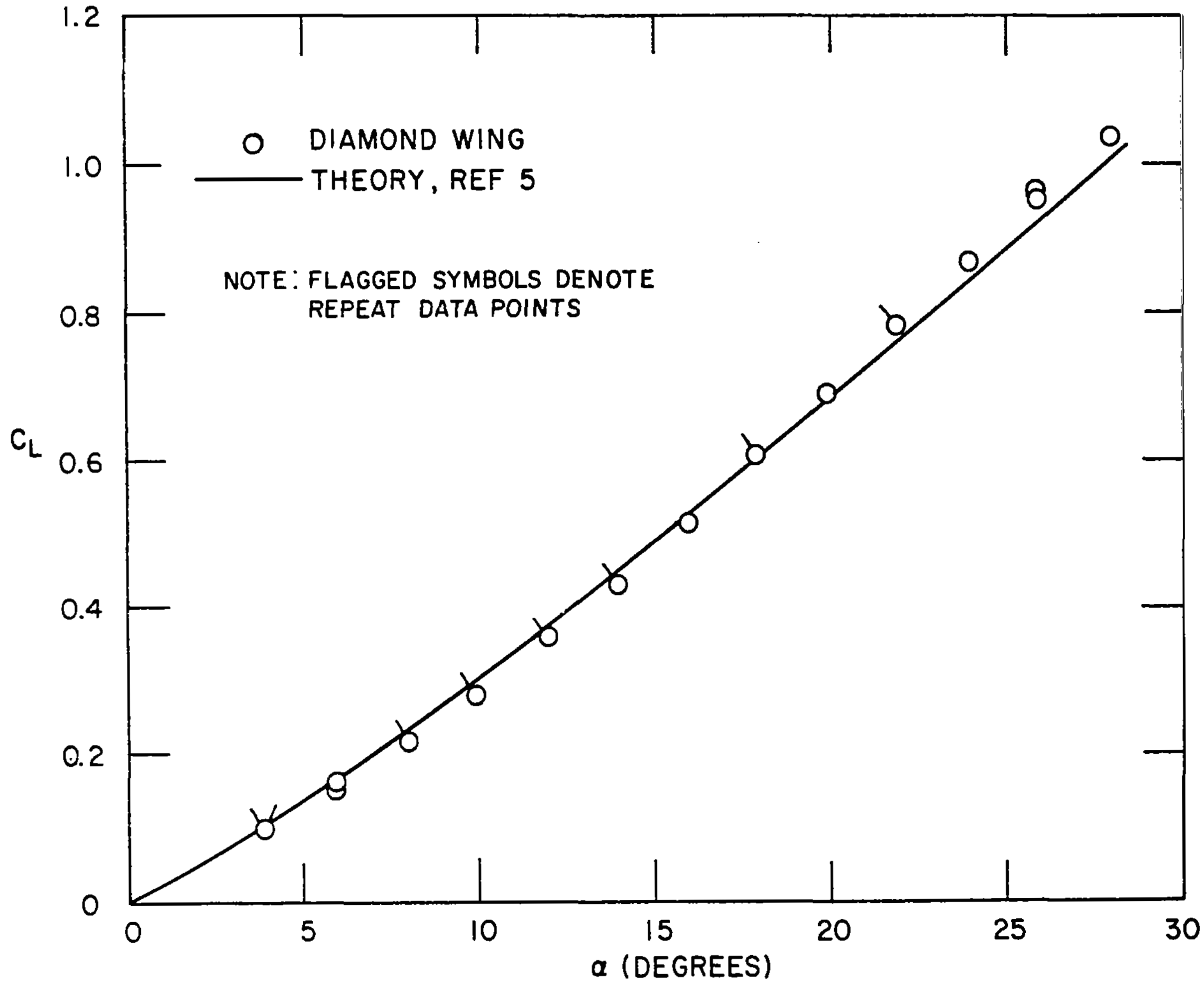

Figure 11. LIFT COEFFICIENT VERSUS ANGLE OF ATTACK

NASA-Langley, 1971 — 1 CR-1796